Analyst

PAPER

View Article Online
View Journal | View Issue

Cite this: *Analyst*, 2014, **139**, 1121

A visible light photoelectrochemical biosensor coupling enzyme-inhibition for organophosphates monitoring based on a dual-functional $Cd_{0.5}Zn_{0.5}S$-reduced graphene oxide nanocomposite

Qian Liu,[ab] Jianrong Cai,[a] Juan Huan,[b] Xiaoya Dong,[b] Chengke Wang,[a] Baijing Qiu[b] and Kun Wang*[b]

Received 30th October 2013
Accepted 5th December 2013

DOI: 10.1039/c3an02044d

www.rsc.org/analyst

A novel visible light photoelectrochemical (PEC) platform coupled with enzyme-inhibition for rapid and sensitive determination of organophosphates (OPs) was constructed based on a dual-functional $Cd_{0.5}Zn_{0.5}S$-reduced graphene oxide ($Cd_{0.5}Zn_{0.5}S$-rGO) nanocomposite. Due to the inherent biocompatibility of the $Cd_{0.5}Zn_{0.5}S$-rGO nanocomposite, acetylcholinesterase (AChE) immobilized on the $Cd_{0.5}Zn_{0.5}S$-rGO modified electrode can hydrolyze acetylthiocholine chloride into thiocholine, which could increase the photocurrent of the enzyme electrode, and the further inhibition of OPs on the enzyme electrode could decrease the photocurrent response. Based on the notable change in the PEC response of the AChE–$Cd_{0.5}Zn_{0.5}S$-rGO modified electrode and using Dursban as a model, a simple and effective way for PEC monitoring of OPs is proposed, which showed a wide linear range of 0.001–1 μg mL^{-1} with a low detection limit of 0.3 ng mL^{-1} ($S/N = 3$). Moreover, the biosensor was successfully challenged with water samples, demonstrating a new method for rapid and sensitive screening/evaluating exposure to organophosphorus pesticides and other hazardous substances.

Introduction

As highly sensitive and selective tools, biosensors can be used as a disposable technique in organophosphates (OPs) monitoring and thus overcome the shortcomings of the conventional chromatographic methods for OPs determination, such as being time-consuming, expensive, not suitable for rapid analysis under field conditions, and requiring to be performed by a highly trained technician.[1,2] Different types of OP biosensors with inherent advantages have been reported in recent years, including organophosphorus hydrolase-based biosensors,[3,4] enzyme-inhibition-based biosensors,[5–7] immunosensors,[8] enzymeless photoelectrochemical (PEC) biosensors,[9,10] *etc.* Among these biosensors, acetylcholinesterase (AChE)-inhibition-based ones have shown satisfactory results for pesticide analysis, where the enzyme activity was employed as an indicator of quantitative measurement of insecticides.[7,11] PEC biosensors exhibit some advantages of both optical methods and electrochemical sensors by coupling irradiation with electrochemical detection, thus favoring promising analytical applications and provoking considerable interest.[12] By using the advantages of PEC biosensors coupled with AChE-inhibition-based biosensors, fabricating a novel PEC-enzyme coupling platform for rapid and sensitive determination of OPs is our dream, which is scarcely reported to date.

As important multifunctional semiconductors, CdS nanocrystals (NCs) incorporated with various nanomaterials have generated great fundamental and technical interest in various fields from biosensors to environment monitoring.[10,13–17] For example, according to Li's group,[13] a CdTe–CdS core–shell quantum dot was utilized as an ultrafast electron transfer relay for improving electron transfer between an electrode and aqueous phase, and a glucose biosensor with high sensitivity, low detection limit, and fast response time was further fabricated. In our previous work,[15] the direct electron transfer between glucose oxidase and a modified electrode was easily achieved due to the distinct advantages of graphene–CdS nanocomposites in enzyme adsorption and bioactivity. Furthermore, the CdS NC-based nanocomposites showed wide applications in the field of PEC sensors. Based on the graphene–CdS nanocomposites, Zhao *et al.* fabricated a PEC biosensor for glutathione detection with a rapid response, wide linear range, and rather low detection limit.[18] By using the remarkable PEC property of phthalocyanine-sensitized graphene–CdS

[a]*School of Food and Biological Engineering, Jiangsu University, Zhenjiang, 212013, P. R. China*

[b]*Key Laboratory of Modern Agriculture Equipment and Technology, School of Chemistry and Chemical Engineering, Jiangsu University, Zhenjiang, 212013, P. R. China. E-mail: wangkun@ujs.edu.cn; Fax: +86 511 88791708; Tel: +86 511 88791800*

nanocomposites, an efficient PEC immunosensing platform for the ultrasensitive detection of the prostate-specific antigen was further presented by this group.[19] All these results above indicate that CdS NC-based composites show great potential in many fields of analytical science; however, to the best of our knowledge, reports on PEC determination of OPs based on CdS NC-based composites have not been reported yet.

Most recently, in order to improve the PEC property of CdS NCs, a series of $Cd_xZn_{1-x}S$/reduced graphene oxide ($Cd_xZn_{1-x}S$/rGO) nanocomposites were prepared by a facile one-pot reaction in our work,[20] and the PEC results indicated that the $Cd_{0.5}Zn_{0.5}S$/rGO nanocomposites exhibited a larger photocurrent response than pure CdS NCs, ZnS NCs and other $Cd_xZn_{1-x}S$/rGO nanocomposites with different x values. Based on the investigation above, herein, a novel PEC platform coupling enzyme-inhibition for determination of OPs was fabricated. Based on the inherent PEC property of $Cd_{0.5}Zn_{0.5}S$/rGO and the efficient inhibition of OPs on the immobilized AChE, a sensitive biosensor for OPs detection was successfully fabricated, which showed good performance in OPs monitoring with a rapid response and low detection limit.

Experimental

Reagents

Acetylcholinesterase (AChE, Type C3389, 500 U mg^{-1} from electric eel), acetylthiocholine chloride (ATCl) and Dursban (100 μg mL^{-1} in methanol) were purchased from Sigma-Aldrich (USA). The $Cd_{0.5}Zn_{0.5}S$-rGO nanocomposite was synthesized and characterized in our previous work.[20] PBS (0.1 M) solutions of various pH values were prepared by mixing stock standard solutions of NaH_2PO_4 and Na_2HPO_4, and adjusting the pH values using 0.1 M H_3PO_4 or NaOH. All solutions were prepared with twice-distilled water.

Apparatus

All electrochemical and PEC measurements were performed with a CHI660 B electrochemical analyzer (Chen Hua Instruments, Shanghai, China), and all experiments were carried out at room temperature (*ca.* 25 °C) with a conventional three-electrode system where a glassy carbon electrode (GCE, 3 mm in diameter) was used as the working electrode, a Ag/AgCl (saturated KCl solution) as the reference electrode and platinum wire as the counter electrode, respectively. The PEC measurements were performed in 0.1 M PBS at 0.3 V, and a 250 W Xe lamp (CHF-XM35-500W, Beijing Chang Tuo) was used as the visible light source with an intensity (passing through a 400 nm UV-cut filter) of 100 mW cm^{-2}. Electrochemical impedance spectroscopy (EIS) was performed in a 0.1 M KCl solution containing 5 mM $Fe(CN)_6^{3-/4-}$ with a frequency range of 0.01 Hz to 10 kHz, and the amplitude of the applied sine wave potential in each case was 5 mV which was taken with a ZENNIUM electrochemical workstation (Zahner Instruments, Germany).

Fabrication of the modified electrode

Prior to modification, the GCE was first polished with sand paper followed by 1.0, 0.3, and 0.05 μm alumina slurry, respectively, and then sonicated in a water bath to remove any residues. 1 mg of the $Cd_{0.5}Zn_{0.5}S$-rGO nanocomposite was dispersed in 0.5 mL twice-distilled water to make a $Cd_{0.5}Zn_{0.5}S$-rGO homogeneous suspension, and then 6 μL of the suspension was cast on the pretreated GCE surface and dried in air at room temperature to form a $Cd_{0.5}Zn_{0.5}S$-rGO modified GCE (denoted as $Cd_{0.5}Zn_{0.5}S$-rGO/GCE). The obtained electrode was finally coated with 4 μL AChE solution (293 U mL^{-1}) and incubated at 25 °C for 30 min. After evaporation of water, the modified electrode was washed with 0.1 M PBS to remove the unbound AChE, and the resulted AChE–$Cd_{0.5}Zn_{0.5}$S-rGO/GCE was stored at 4 °C when not in use.

PEC determination of OPs under visible light irradiation

For the measurement of Dursban as the model of OPs, the obtained AChE–$Cd_{0.5}Zn_{0.5}S$-rGO/GCE was first immersed in 0.1 M PBS (pH 7.0) containing different concentrations of standard Dursban for 6 min, and then transferred to the electrochemical cell of 5.0 mL PBS (pH 7.0) containing 0.6 mM ATCl, an enzyme substrate, to study the PEC response. For comparison, the PEC responses were also recorded by immersing the AChE–$Cd_{0.5}Zn_{0.5}S$-rGO/GCE in 0.1 M PBS containing 0.6 mM ATCl for 6 min in the absence of Dursban.

Results and discussion

EIS of the modified electrodes

By using $[Fe(CN)_6]^{3-/4-}$ as the redox probe, the Nyquist plots of different electrodes were investigated in the frequency range of 10^{-2} to 10^5 Hz. As shown in Fig. 1, the bare GCE presented a charge-transfer resistance (R_{ct}) value of 90 Ω with an almost straight tail line (curve *a*), indicating the characteristic of a diffuse limiting step of the electrochemical process.[21] After the immobilization of $Cd_{0.5}Zn_{0.5}S$-rGO on the electrode surface, an increase of R_{ct} (170 Ω) was observed (curve *b*), which was due to the incorporation of the $Cd_{0.5}Zn_{0.5}S$-rGO nanocomposite. However, after AChE was immobilized on the electrode, the R_{ct} value increased up to 2300 Ω (curve *c*), which was attributed to the fact that most biological molecules, including enzymes, are poor electrical conductors at low frequencies and cause hindrance

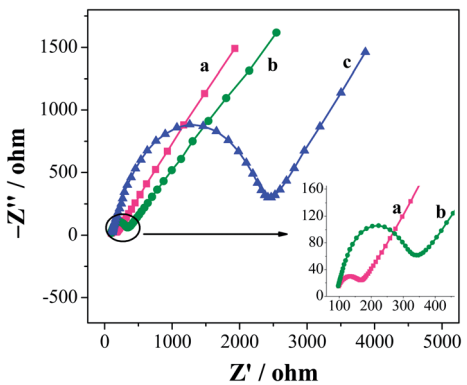

Fig. 1 EIS of bare GCE (a), $Cd_{0.5}Zn_{0.5}S$-rGO/GCE (b) and AChE–$Cd_{0.5}Zn_{0.5}S$-rGO/GCE (c) in 0.1 M KCl containing 5 mM $Fe(CN)_6^{3-/4-}$. Inset: the enlarged EIS of bare GCE (a) and $Cd_{0.5}Zn_{0.5}S$-rGO/GCE (b).

to the electron transfer,[5] and this was the direct evidence of successful binding of the enzyme on the electrode surface.

PEC behaviors of the modified electrodes

The PEC behaviors of different modified electrodes were investigated in 0.1 M PBS (pH 7.0) under visible irradiation. As can be seen in Fig. 2, no obvious photocurrent was observed at bare GCE under visible light irradiation (curve *a*), and the photocurrent signal at both the $Cd_{0.5}Zn_{0.5}S$-rGO/GCE (curve *b*) and the AChE–$Cd_{0.5}Zn_{0.5}S$-rGO/GCE (curve *c*) increased greatly, which was due to the integration of the $Cd_{0.5}Zn_{0.5}S$-rGO nanocomposite. In addition, compared with the $Cd_{0.5}Zn_{0.5}S$-rGO/GCE, it was clear that the photocurrent response of the AChE–$Cd_{0.5}Zn_{0.5}S$-rGO/GCE slightly enhanced with the introduction of AChE, which was probably due to the light-harvesting effect of AChE toward visible light as well as the permission of electron or energy migration between AChE and the $Cd_{0.5}Zn_{0.5}S$-rGO nanocomposite.[22] More interestingly, a significantly enhanced photocurrent in the AChE–$Cd_{0.5}Zn_{0.5}S$-rGO film (curve *d*) was observed with the further addition of ATCl to the electrolyte, which could be explained as follows: when this system is exposed to a solution containing ATCl, the immobilized AChE can hydrolyze ATCl into thiocholine and acetate. Upon irradiation, thiocholine acts as a sacrificial electron donor to scavenge the holes and improves the efficiency of charge separation, leading to a prominent increase in the photocurrent.[23]

Optimization for the PEC responses at the AChE–$Cd_{0.5}Zn_{0.5}S$-rGO/GCE

In order to achieve the optimal PEC response for OPs determination, effects of solution pH, ATCl concentration and inhibition time on the PEC behaviors of the AChE–$Cd_{0.5}Zn_{0.5}S$-rGO modified electrode were considered carefully.

The effect of solution pH on the PEC behavior of the AChE–$Cd_{0.5}Zn_{0.5}S$-rGO/GCE was determined in 0.1 M PBS with the pH range of 5.0–9.0. As shown in Fig. 3A, the photocurrent increased slowly with the increase of pH from 5.0 to 6.0 and then decreased slightly with the pH from 6.0 to 9.0, indicating that the AChE–$Cd_{0.5}Zn_{0.5}S$-rGO modified electrode exhibited a relatively stable PEC signal in a wide pH range. However, in order to keep the bioactivity of AChE on the AChE–$Cd_{0.5}Zn_{0.5}S$-rGO film, pH 7.0 was selected in the subsequent experiment.

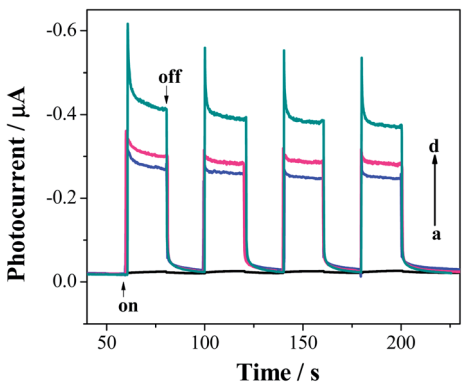

Fig. 2 The photocurrent responses of bare GCE (a), $Cd_{0.5}Zn_{0.5}S$-rGO/GCE (b), and AChE–$Cd_{0.5}Zn_{0.5}S$-rGO/GCE (c) in 0.1 M PBS (pH 7.0), and AChE–$Cd_{0.5}Zn_{0.5}S$-rGO/GCE in 0.1 M PBS (pH 7.0) containing 0.6 mM ATCl.

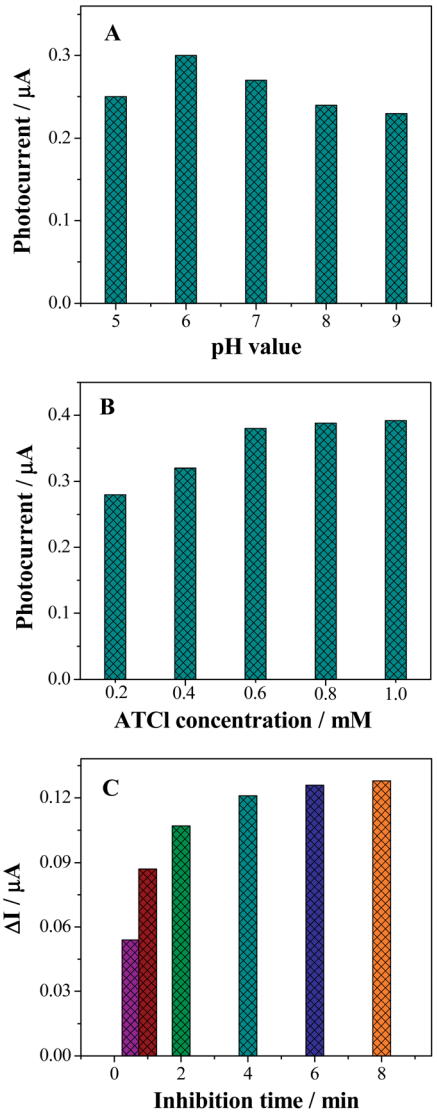

Fig. 3 Effects of solution pH (A), ATCl concentration (B) and inhibition time of 10 ng mL^{-1} Dursban (C) on the photocurrent responses of the AChE–$Cd_{0.5}Zn_{0.5}S$-rGO/GCE.

The ATCl concentration is one of the most influential parameters; when the concentration of ATCl is too low, the photocurrent generated by the enzyme electrode is too small that the determination of OPs is hardly feasible; however, too high ATCl concentration would cause all the active centers of AChE being occupied by the substrate and insensible to the inhibitor.[22] Therefore, the effect of ATCl concentration on the photocurrent responses of the AChE–$Cd_{0.5}Zn_{0.5}S$-rGO film was considered carefully in our work. As shown in Fig. 3B, the photocurrent increased gradually with the increase of the ATCl concentration, however, when the concentration of ATCl reached 0.6 mM, the photocurrent increased slowly and tended to a stable signal. Thus, 0.6 mM was chosen as the optimal concentration of ATCl in this experiment.

Table 1 Comparison of the as-prepared biosensor for detection of pesticides with other AChE-based or PEC-based biosensors

Electrode	Linear range (μg mL^{-1})	Detection limit (ng mL^{-1})	Response time (min)	References
PEC-based biosensor				
P3HT[a]/TiO_2/GCE	0.07–5.6	3.5	—	9
PoPD[b]-AuNPs[c]/TiO_2 NTs electrode	0.017–3.5	0.3	—	12
Nanometer-sized titania/SPE[d]	0.006–0.03, 0.06–0.32	0.6	—	24
AChE-based biosensor				
AChE-Er-GRO[e]- Nafion/GCE	0.005–0.1, 3–20	2.0	10	6
AChE-BiOINFs[f]/ITO	0.001–0.08, 0.3–1.0	0.04	12	22
AChE–$Cd_{0.5}Zn_{0.5}$S-rGO/GCE	0.001–1	0.3	6	This work

[a] Poly(3-hexylthiophene). [b] Poly(*o*-phenylenediamine). [c] Au nanoparticles. [d] Screen-printed electrode. [e] Electrochemically reduced graphene oxide. [f] Crossed bismuth oxyiodide nanoflake arrays.

The inhibition time is an important parameter in pesticide analysis, therefore, the dependence of inhibition time on the Dursban inhibition was also investigated. As can be noted in Fig. 3C, Dursban displayed an increasing inhibition on AChE with the inhibition time increased, and when the inhibition time was longer than 6 min, the inhibition tended to a stable value, indicating that the binding interaction with active target groups in the enzyme reached saturation. Thus, 6 min inhibition time was used in our experiment. In addition, the inhibition time obtained in this work was relatively small compared to previous reports as shown in Table 1, and based on the above results, a rapid method for Dursban detection was successfully proposed.

Analytical performance for PEC determination of OPs

Based on the inhibition of OPs on the immobilized AChE activity and selecting Dursban as a model, a simple and effective way for PEC monitoring of OPs is proposed in Fig. 4. It was obvious that the photocurrent decreased gradually with the increase of Dursban concentration (Fig. 4A), and the ΔI ($I_0 - I$, I_0 is the initial photocurrent of the AChE–$Cd_{0.5}Zn_{0.5}$S-rGO/GCE, and I is the photocurrent of the enzyme electrode after Dursban inhibition) was linearly dependent on the logarithm of Dursban concentration in the range of 0.001–1 μg mL^{-1} with a detection limit of 0.3 ng mL^{-1} ($S/N = 3$) (Fig. 4B), indicating that the proposed dual-functional film is remarkably reliable for the sensitive determination of OPs. In addition, the as-prepared PEC-enzyme coupling platform shows a wider linear range and a comparable or lower detection limit for OPs detection than other AChE-based or PEC-based biosensors in previous reports, as shown in Table 1.

The detection mechanism for OPs based on the AChE–$Cd_{0.5}Zn_{0.5}$S-rGO modified electrode

Scheme 1 intuitively shows the procedure of AChE–$Cd_{0.5}Zn_{0.5}$S-rGO/GCE preparation and the mechanism for the PEC determination of OPs based on the PEC biosensor. Due to the inherent biocompatibility and PEC property of the $Cd_{0.5}Zn_{0.5}$S-rGO nanocomposite, the immobilized AChE can hydrolyze ATCl into thiocholine and acetate, and upon irradiation, thiocholine acts as a sacrificial electron donor to scavenge the holes and improves the efficiency of charge separation, leading to a prominent increase in the photocurrent of the modified enzyme electrode;[23] however, when inhibited by OPs, the inhibitors bind to the esterase active site of AChE and thus inhibit its catalytic activity, hindering the production of electron and resulting in the decrease of the photocurrent response.[22] Therefore, due to the notable change in the PEC signal of the AChE–$Cd_{0.5}Zn_{0.5}$S-rGO modified electrode,

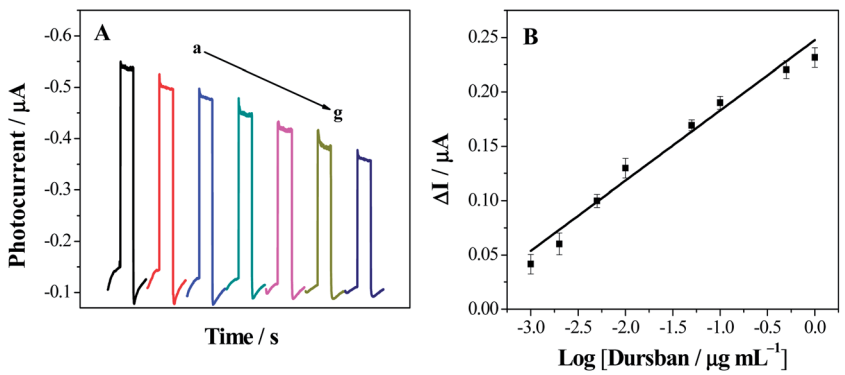

Fig. 4 (A) The photocurrent responses of the AChE–$Cd_{0.5}Zn_{0.5}$S-rGO/GCE in 0.1 M PBS (pH 7.0) containing 0.6 mM ATCl after incubation in (a) 0, (b) 0.001, (c) 0.002, (d) 0.005, (e) 0.01, (f) 0.05 and (g) 0.1 μg mL^{-1} Dursban solution for 6 min. (B) The calibration curve for Dursban determination. Error bars: ±S.D., $n = 5$.

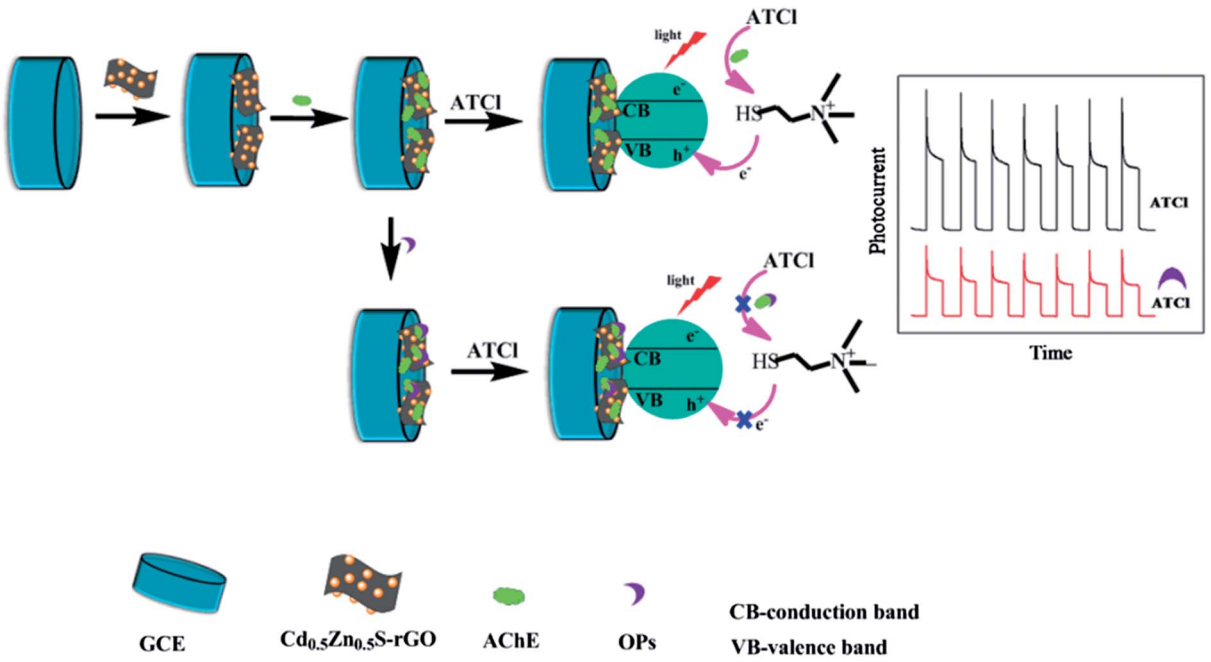

Scheme 1 Illustration of the procedure of AChE–$Cd_{0.5}Zn_{0.5}S$-rGO/GCE preparation and the PEC mechanism for OPs determination.

the intriguing applications of dual-functional $Cd_{0.5}Zn_{0.5}S$-rGO for PEC biosensing of OPs under visible light irradiation could be fabricated.

Stability, reproducibility, selectivity and real sample analysis

The PEC stability of the AChE–$Cd_{0.5}Zn_{0.5}S$-rGO/GCE was also investigated in 0.1 M PBS (pH 7.0) in the presence of 0.6 mM ATCl. As shown in Fig. 5A, the PEC response of the AChE–$Cd_{0.5}Zn_{0.5}$-S-rGO/GCE was repeated 10 times every 40 s under visible irradiation, and the photocurrent response was *ca.* 0.5 μA and did not show any obvious change. The relative standard deviation (RSD) was only 1.76%, which indicated that the photocurrent response of the modified electrode was stable and beneficial for the fabrication of a PEC biosensor. When the enzyme electrode was not in use, it was stored at 4 °C under dry conditions. No obvious decrease in the photocurrent response of ATCl was observed in the first 7 day storage, after a 20 day storage period, the sensor retained 88% of its initial photocurrent response (data not shown), indicating the acceptable long-term stability of the PEC biosensor. Furthermore, the reproducibility of the PEC sensor was estimated at five different electrodes, and the RSD was found to be 9.3%, indicating acceptable reproducibility.

To demonstrate the practicality of the proposed biosensor, a recovery test was carried out by adding different amounts of Dursban into tap and river water samples, and the results are presented in Table 2. As can be seen, the results are in agreement with the given concentrations with average recoveries from 92.0% to 105.2% ($n = 4$), and the results deviate from the given concentrations of Dursban in the samples maybe resulting from the accuracy of the calibration plots of the PEC biosensor and the possible interference species that co-exist in

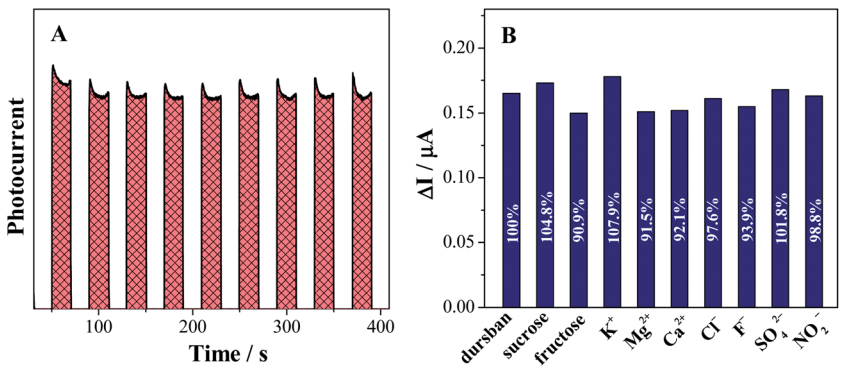

Fig. 5 (A) Time-based photocurrent response of the AChE–$Cd_{0.5}Zn_{0.5}S$-rGO/GCE in 0.1 M PBS (pH 7.0) containing 0.6 mM ATCl under visible irradiation repeated every 40 s; (B) interference of sucrose, fructose, K^+, Mg^{2+}, Ca^{2+}, Cl^-, F^-, SO_4^{2-} and NO_2^- separately on the Δ*I* of the AChE–$Cd_{0.5}Zn_{0.5}S$-rGO/GCE in 0.1 M PBS (pH 7.0) containing 0.6 mM ATCl after incubated with 0.05 μg mL^{-1} Dursban.

Table 2 Recovery studies of Dursban in tap and river water samples ($n = 4$)

Sample	Taken (ng mL^{-1})	Found (ng mL^{-1})	Recovery (%)	RSD (%)
Tap water	0.00	Not detected	—	—
	10.0	9.2	92.0	4.6
	50.0	52.3	104.6	5.3
	100	98.5	98.5	3.4
River water	0.00	Not detected	—	—
	10.0	10.4	104	5.2
	50.0	47.7	105.2	3.7
	100	104.3	104.3	6.2

the samples. These results indicate that this new method could be used for analysis of real samples.

In addition, the PEC signal for 0.6 mM ATCl was compared with the signal obtained in the presence of the interference species. As shown in Fig. 5B, the possible interference species which may have coexisted with OPs in food and drinking water such as sucrose and fructose with the concentrations of 8 mM and K^+, Mg^{2+}, Ca^{2+}, Cl^-, F^-, SO_4^{2-} and NO_2^- with the concentrations of 0.05 M were investigated. The interference studies of K^+, Mg^{2+}, Ca^{2+}, Cl^-, F^-, SO_4^{2-} and NO_2^- on the PEC signal were investigated in 0.1 M PBS in the presence of 0.05 M KCl, $MgCl_2$, $CaCl_2$, NaCl, NaF, Na_2SO_4 and $NaNO_2$, respectively. The RSD of the possible interference species on the photocurrent response was found in the range of 90.9% to 107.9%, which indicated that the possible interference species has little effect on the Dursban detection.

Conclusions

In summary, based on the inherent biocompatibility and remarkable PEC property of the dual-functional $Cd_{0.5}Zn_{0.5}S$-rGO nanocomposite, a novel PEC platform coupled with enzyme-inhibition was constructed for OPs determination. The biocatalytic activity of the immobilized AChE can be effectively maintained due to the inherent biocompatibility of $Cd_{0.5}Zn_{0.5}S$-rGO, and the remarkable PEC property can provide the platform for sensitive detection of the analyte. Due to the notable change in the PEC signal of the AChE–$Cd_{0.5}Zn_{0.5}S$-rGO modified electrode, the intriguing applications of dual-functional $Cd_{0.5}Zn_{0.5}S$-rGO for PEC sensing of OPs under visible light irradiation were fabricated. The PEC biosensor exhibited excellent performance on the merits of a wide linear range, low detection limit, short response time, good stability and reproducibility. In addition, satisfactory results were obtained when the biosensor was challenged with water samples, which would hold a new perspective to apply the PEC-enzyme coupling system in pesticide determination.

Acknowledgements

The present work was supported by the National Natural Science Foundation of China (nos 21175061, 21375050, 21305052, 21305032 and 31271620), Program of Natural Science Foundation of Education Bureau of Jiangsu Province, China (grant nos 10KJA470007 and 13KJB210004), Key Laboratory of Modern Agriculture Equipment and Technology (no. NZ201109), China Postdoctoral Science Foundation (no. 2012M511217), and Innovation Project of Science and Technology for College Graduates of Jiangsu Province (no. CXZZ12_0704).

References

1 M. M. Liang, K. L. Fan, Y. Pan, H. Jiang, F. Wang, D. L. Yang, D. Lu, J. Feng, J. J. Zhao, L. Yang and X. Y. Yan, *Anal. Chem.*, 2013, **85**, 308–312.
2 S. Q. Liu, Z. Z. Zheng and X. Y. Li, *Anal. Bioanal. Chem.*, 2013, **405**, 63–90.
3 Y. T. Zhao, W. Y. Zhang, Y. H. Lin and D. Du, *Nanoscale*, 2013, **5**, 1121–1126.
4 A. Sahin, K. Dooley, D. M. Cropek, A. C. West and S. Banta, *Sens. Actuators, B*, 2011, **158**, 353–360.
5 N. Chauhan, J. Narang and C. S. Pundir, *Biosens. Bioelectron.*, 2011, **29**, 82–88.
6 S. Wu, F. F. Huang, X. Q. Lan, X. Y. Wang, J. M. Wang and C. G. Meng, *Sens. Actuators, B*, 2013, **177**, 724–729.
7 K. Wang, Q. Liu, L. N. Dai, J. J. Yan, C. Ju, B. J. Qiu and X. Y. Wu, *Anal. Chim. Acta*, 2011, **695**, 84–88.
8 Z. L. Xu, Y. D. Shen, W. X. Zheng, R. C. Beier, G. M. Xie, J. X. Dong, J. Y. Yang, H. Wang, H. T. Lei, Z. G. She and Y. M. Sun, *Anal. Chem.*, 2010, **82**, 9314–9321.
9 H. B. Li, J. Li, Q. Xu and X. Y. Hu, *Anal. Chem.*, 2011, **83**, 9681–9686.
10 H. B. Li, J. Li, Q. Xu, Z. J. Yang and X. Y. Hu, *Anal. Chim. Acta*, 2013, **766**, 47–52.
11 G. D. Liu and Y. H. Lin, *Anal. Chem.*, 2006, **78**, 835–843.
12 P. P. Wang, W. J. Dai, L. Ge, M. Yan, S. G. Ge and J. H. Yu, *Analyst*, 2013, **138**, 939–945.
13 Z. G. Gu, S. P. Yang, Z. J. Li, X. L. Sun, G. L. Wang, Y. J. Fang and J. K. Liu, *Electrochim. Acta*, 2011, **56**, 9162–9167.
14 W. W. Zhao, Z. Y. Ma, D. Y. Yan, J. J. Xu and H. Y. Chen, *Anal. Chem.*, 2012, **84**, 10518–10521.
15 K. Wang, Q. Liu, Q. M. Guan, J. Wu, H. N. Li and J. J. Yan, *Biosens. Bioelectron.*, 2011, **26**, 2252–2257.
16 E. Golub, G. Pelossof, R. Freeman, H. Zhang and I. Willner, *Anal. Chem.*, 2009, **81**, 9291–9298.
17 Q. M. Shen, X. M. Zhao, S. W. Zhou, W. H. Hou and J. J. Zhu, *J. Phys. Chem. C*, 2011, **115**, 17958–17964.
18 X. M. Zhao, S. W. Zhou, Q. M. Shen, L. P. Jiang and J. J. Zhu, *Analyst*, 2012, **137**, 3697–3703.
19 Y. J. Li, M. J. Ma, G. Yin, Y. Kong and J. J. Zhu, *Chem.–Eur. J.*, 2013, **19**, 4496–4505.
20 J. J. Yan, K. Wang, Q. Liu, J. Qian, X. Y. Dong, W. Liu and B. J. Qiu, *RSC Adv.*, 2013, **3**, 14451–14457.
21 D. Du, W. J. Chen, W. Y. Zhang, D. L. Liu, H. B. Li and Y. H. Lin, *Biosens. Bioelectron.*, 2010, **25**, 1370–1375.
22 J. M. Gong, X. Q. Wang, X. Li and K. W. Wang, *Biosens. Bioelectron.*, 2012, **38**, 43–49.
23 V. Pardo-Yissar, E. Katz, J. Wasserman and I. Willner, *J. Am. Chem. Soc.*, 2003, **125**, 622–623.
24 H. B. Li, J. Li, Z. J. Yang, Q. Xu and X. Y. Hu, *Anal. Chem.*, 2011, **83**, 5290–5295.

